 doi:10.20944/preprints202008.0055.v1

*Article*

# IIAEK Targets Intestinal Alkaline Phosphatase (IAP) to Improve Cholesterol Metabolism with a Specific Activation of IAP and Down-Regulation of ABCA1

**Asahi Takeuchi [1,†], Kentaro Hisamatsu [1,†], Natsuki Okumura [1], Yuki Sugimitsu [1], Emiko Yanase [2], Yoshihito Ueno [2] and Satoshi Nagaoka [1,*]**

[1] Laboratory of Molecular Function of Food, Department of Applied Life Science, Faculty of Applied Biological Sciences, Gifu University, 1-1 Yanagido, Gifu 501-1193, Japan; z4521051@edu.gifu-u.ac.jp (A.T.); 8polonium4@gmail.com (K.H.); natsunatsu11294@gmail.com (N.O.); nome.imakev.og@gmail.com (Y.S.)

[2] Laboratory of Bio-organic Chemistry, Department of Applied Life Science, Faculty of Applied Biological Sciences, Gifu University, 1-1 Yanagido, Gifu 501-1193, Japan; e-yanase@gifu-u.ac.jp (E.Y.); uenoy@gifu-u.ac.jp (Y.U.)

* Correspondence: nagaoka@gifu-u.ac.jp; Tel.: +81-58-293-2931

† these authors contributed equally to this work.

**Abstract:** IIAEK (Ile-Ile-Ala-Glu-Lys, lactostatin) is a novel pentapeptide from bovine milk β-lactoglobulin which lowers cholesterol levels. However, the molecular mechanisms underlying the suppression of intestinal cholesterol absorption by IIAEK are unknown. Therefore, we evaluated the effects of IIAEK on intestinal cholesterol metabolism in Caco-2 cells in a human intestinal model. We found that IIAEK significantly reduced the expression of intestinal cholesterol metabolism-associated genes, particularly that of the ATP-binding cassette transporter A1 (ABCA1) protein. Subsequently, we chemically synthesized a novel molecular probe, IIXEK, which can visualize a complex of target proteins interacting with photoaffinity-labeled IIAEK by fluorescent substances. Photoaffinity labeling and MS analysis with IIXEK for the rat small intestinal mucosa and intestinal lipid raft fractions of Caco-2 cells, we identified intestinal alkaline phosphatase (IAP) as a specific molecule interacting with IIAEK and discovered IIAEK common binding amino acid sequence, GFYLFVEGGR. Transfection of IAP siRNA counteracted the decrease in ABCA1 mRNA levels in Caco-2 cells. IIAEK significantly increased IAP mRNA and protein levels, and significantly decreased ABCA1 mRNA and protein levels in Caco-2 cells. In conclusion, we found that IIAEK targets IAP to improve cholesterol metabolism via a novel signaling pathway with a specific activation of IAP and down-regulation of intestinal ABCA1.

**Keywords:** IIAEK; IAP; photoaffinity labeling; click reaction; Caco-2 cells; cholesterol; ABCA1

## 1. Introduction

Lifestyle diseases, especially arteriosclerosis-related disorders, are closely associated with diet. Improving cholesterol metabolism by diet modification is an important strategy for preventing or improving hypercholesterolemia and hyperlipidemia [1]. Dietary proteins and peptides are effective in ameliorating dyslipidemia and hypercholesterolemia in animals and humans [2]. However, the molecular mechanisms underlying their cholesterol-lowering effect has not been elucidated. Previously we had discovered a cholesterol metabolism-improving pentapeptide - IIAEK (lactostatin). It was obtained from β-lactoglobulin trypsin hydrolysate (LTH), a major component of the whey protein of milk [3]. We found that the serum cholesterol-lowering effect of IIAEK is comparable to that of beta-sitosterol, a phytosterol that was marketed as a pharmaceutical product in an oral study in rats [3]. Since cholesterol is converted to bile acids and excreted in the liver, the effects of IIAEK on cholesterol 7alpha-hydroxylase (CYP7A1), a rate-limiting enzyme in bile acid synthesis, was evaluated. Modulation of CYP7A1 gene expression, which is crucial for the prevention

 doi:10.20944/preprints202008.0055.v1



and improvement of hyperlipidemia and atherosclerosis, has been reported to improve these conditions in model animals overexpressing CYP7A1 [4,5]. The addition of IIAEK to HepG2 cells, which are human hepatocarcinoma-derived cells, significantly increased their CYP7A1 mRNA levels relative to the control [6]. In addition, the IIAEK-induced upregulation of CYP7A1 mRNA was triggered by the promotion of its transcriptional activity by the calcium channel-mediated MAPK signaling pathway [6]. We proposed that IIAEK might improve cholesterol metabolism via a specific membrane protein (e.g. membrane receptor) recognized by IIAEK in HepG2 cells [6]. Interestingly, IIAEK is not degraded by digestive enzymes like pepsin and trypsin. Therefore, it reaches the small intestine prior to intestinal absorption. However, the way in which IIAEK directly affects the small intestinal epithelium is unclear. Our hypothesis is that the target protein (such as receptor) of IIAEK is associated with a novel regulatory pathway responsible for intestinal cholesterol metabolism. There is no information about food-derived bioactive peptide related specific receptor including IIAEK.

Therefore, in the present study, photoaffinity labeling was performed to visualize the target proteins interacting with IIAEK, and fluorescent labeled probes were synthesized chemically to capture the target proteins. Photoaffinity labeling, a technique developed by Westheimer in 1962, utilizes the reversible interaction of a bioactive compound with a target protein [7]. Generally, protein-ligand interactions are characterized by transient, non-covalent interactions. However, in photoaffinity labeling, transient protein-ligand interactions are analyzed by the formation of covalent complexes with photoreactive groups, thereby enabling the identification of the interacting amino acid sequences [8]. In addition, we utilized the click reaction to visualize the photoaffinity-labeled target protein-IIAEK complex. The click reaction, proposed by Sharpless *et al.*, is a covalent bond-forming reaction that functions effectively during molecular modifications and coupling reactions [9]. The best-known click reaction is the cycloaddition of azides and alkynes (Huisgen cycloaddition) reported by Sharpless *et al*. [10] and Meldal *et al.* [11]. In photoaffinity labeling, first, the ligand-target protein complex is irreversibly covalently cross-linked by UV irradiation. This complex is then labeled with a fluorescent azide (rhodamine) using click reaction, and finally, the fluorescent azide-labeled captured target protein complex is separated and identified using SDS-PAGE and MS, respectively. Collectively, in the present study, we used a human small intestinal epithelial model (Caco-2 cells) to identify the intestinal cholesterol absorption-associated genes affected by IIAEK, with particular attention to ABCA1. In addition, we also performed photoaffinity labeling and MS analysis with the chemically synthesized novel molecular probe, IIXEK, on rat small intestinal mucosal fractions and intestinal lipid raft fractions from Caco-2 cells to identify the target molecules interacting with IIAEK in the small intestinal epithelium. Furthermore, we assessed the relationship between intestinal ABCA1 and IAP（intestinal alkaline phosphatase), the specific molecule interacting with IIAEK in Caco-2 cells.

## 2. Materials and Methods

### *2.1. Cell Culture*

Caco-2 cells were acquired from the American Type Culture Collection (Manassas, USA). The cells were maintained in Dulbecco's modified Eagle's medium (DMEM) supplemented with 10% fetal calf serum, 4 mmol/L l-glutamine, 50,000 IU/L penicillin, and 50 mg/L streptomycin. The cells were either seeded in 6-well Transwell® plates (Corning, Inc., USA) at a density of $2\times10^5$ cells/well or in 75 mm Transwell® plates (Corning, Inc., USA) at a density of $18.8\times10^5$ cells/well, and grown for 14 days post-confluence or for 8 h pre-confluence.

### *2.2. Chemicals*

IIAEK (Ile-Ile-Ala-Glu-Lys ： purity (>95%)) and IIXEK (purity>95%) were obtained from Peptide Institute, Inc (Japan). Cholesterol and sodium taurocholate were purchased from Sigma Aldrich (USA).

 doi:10.20944/preprints202008.0055.v1



*2.3. Cholesterol Absorption Assay for Caco-2 Cells*

Caco-2 cells were grown in 6-well Transwell® plates (Corning, Inc., USA) containing 0.5 mL of fetal bovine serum supplemented with DMEM for 14 days post-confluence. The absorption of [$^{14}$C]-labeled micellar cholesterol in Caco-2 cells was measured for 24 h as described previously [12,13] with some modifications. On day 14, [$^{14}$C]-labeled micellar solutions containing 3.7 kBq [4-$^{14}$C]-cholesterol (2.0 Gbq/mmol, NEN) with or without 2 mM IIAEK, 5 mM taurocholate, and 250 μM cholesterol in serum-free DMEM were prepared by sonication and incubated with shaking at 37℃ for 24 h. Following incubation, cholesterol absorption was measured for 24 h. The cellular protein concentration was determined using a commercially available kit (Bio-Rad Protein Assay; Bio-Rad).

*2.4. RNA Preparation from Caco-2 Cells and Real-Time PCR Using TaqMan Probe*

Caco-2 cells were treated with or without 2 mM IIAEK for 24 h. The micelle for micelle treatment consisted of 5 mM taurocholate and 250 μM cholesterol as described previously [13]. Following treatment, total RNA was isolated from Caco-2 cells using a NucleoSpin® RNA Kit (MACHEREY-NAGEL, Düren, Germany) and treated with DNase I (RNase-Free DNase; Qiagen, 79254). The total RNA was converted to cDNA using a High-Capacity cDNA Archive Kit (Applied Biosystems). Real-time PCR was performed on an ABI PRISM 7000, using TaqMan® Universal PCR Master Mix (Applied Biosystems), according to the manufacturer's protocol, as described previously [14]. TaqMan® Ribosomal RNA Control Reagents (Applied Biosystems) were used as primers and a TaqMan® probe was used for the 18S ribosomal RNA gene-based PCR. The primers and TaqMan® probes for human scavenger receptor B-1 (SR-B1, Hs00969821_m1), Niemann-Pick C1-like 1 (NPC1L1, Ha00203602_m1), ATP-binding cassette transporter A1 (ABCA1, Hs00194045_m1), acetyl-CoA acetyltransferase 2 (ACAT2, Hs00255067_m1), Microsomal triglyceride transfer protein (MTP, Hs00165177_m1), ATP-binding cassette transporter G5 (ABCG5, Hs03037375_m1), ATP-binding cassette transporter G8 (ABCG8, Hs00223690_m1), Cytochrome P450, family 27, subfamily A, polypeptide 1 (CYP27A1, Hs01026016_m1), and 18S ribosomal RNA (4308329) were purchased from Applied Biosystems, as part of a TaqMan® Gene Expression Assay. The following primers were used with the StepOnePlus™ real-time PCR system (Applied Biosystems) and SYBR® Premix Ex Taq (TAKARA): for human SR-B1, TCCTCACTTCCTCAACGCTG (forward) and TCCCAGTTTGTCCAATGCC (reverse); for NPC1L1, ATCTTAACTGTCGGATCCACAAAAA (forward) and AACCTGATGGCATTGTGAGACAT (reverse); for ABCA1, TGCTGCATAGTCTTGGGACTC (forward) and ACCTCCTGTCGCATGTCACT (reverse); for ACAT2, CCGGAAGATGTGTCTGAGGT (forward) and CACCCACACTGGCTTGTCTA (reverse); for MTP, ACCTGCAGACGTGTATTCATTC (forward) and CCCAGCTAGGAGTCACTGAGA (reverse); for ABCG5, CCGACTGATTGGCAACTACA (forward) and GCTCATCAAACAGCATGACC (reverse); for ABCG8, AACTTGAGCAGCCTGTGGA (forward) and CATCAGCCCTTCAAAACACC (reverse); for CYP27A1, GTGCTGCCTTTCTGGAAGCGAT (forward) and TAGCCAGACACCTGGATGCCAT (reverse);and for 18S ribosomal RNA, CTCAACACGGGAAACCTCAC (forward) and CGCTCCACCAACTAAGAACG (reverse).

*2.5. RNA Preparation from Caco-2 Cells and Real-Time PCR*

Caco-2 cell treatment, and RNA and cDNA preparations were performed as described previously [12]. Real-time PCR was performed using a StepOnePlus™ Real-time PCR system (Applied Biosystems) and SYBR® Premix Ex Taq (TAKARA), according to the manufacturer's protocol. The following primers were used in the assay: for ABCA1, TGCTGCATAGTCTTGGGACTC (forward) and ACCTCCTGTCGCATGTCACT (reverse); for intestinal alkaline phosphatase (IAP), CATACCTGGCTCTGTCCAAGA (forward) and GTCTGGAAGTTGGCCTTGAC (reverse); for Liver X receptor α (LXRα), TGGACACCTACATGCGTCGCAA (forward) and CAAGGATGTGGCATGAGCCTGT (reverse); for Liver X receptor β (LXRβ), CTTCGCTAAGCAAGTGCCTGGT (forward) and CACTCTGTCTCGTGGTTGTAGC (reverse);

 doi:10.20944/preprints202008.0055.v1



and for 18S ribosomal RNA, CTCAACACGGGAAACCTCAC (forward) and CGCTCCACCAACTAAGAACG (reverse).

### *2.6. Western Blot Analysis of Caco-2 Cells*

Caco-2 cells were treated with or without 2 mM IIAEK for 48 h for ABCA1 protein level with cholesterol micelle or 24h for IAP and ABCA1 protein levels. The micelle was prepared as described previously [13]. Protein preparation from Caco-2 cells and Western blot analyses were performed as described previously [12]. For Western blot analysis, we used the following specific antibodies: anti-ABCA1 (sc-58219, Santa Cruz Biotechnology), anti-IAP (ab184622, abcam), and anti-β-actin (sc-47778, Santa Cruz). Western blot analyses were performed using an ImmunoStar® LD system (Wako Pure Chemical Industries).

### *2.7. Transient Transfections and Luciferase Assay Using Caco-2 Cells*

Protein preparation from Caco-2 cells and luciferase analyses were performed as described previously [12]. Following plasmid (ABCA1-Luc plasmid containing −928 to ＋107 bp, −536 to ＋107 bp, −126 to ＋107 bp, or −36 to ＋107 bp of the ABCA1 gene promoter, and pPGK β-galactosidase plasmid) transfection, the cells were incubated with 2 mM IIAEK for 12 h with micelle which were prepared as described previously [13]. Subsequently, the cells were lysed with reporter lysis buffer (Promega, Madison, USA). Luciferase activity was measured using a luciferase assay system (Promega) on a Fluoroskan Ascent FL instrument (Labsystems) according to the manufacturer's instructions. β-Galactosidase activity was measured using a β-galactosidase ELISA Kit (Promega) and normalized to the luciferase activity.

### *2.8. Intestinal Alkaline Phosphatase Measurement*

Intestinal alkaline phosphatase（IAP）measurement was performed as described previously [15,16] with some modifications. Caco-2 cells were treated with or without 2 mM IIAEK. The micelle was prepared as described previously [13]. Following treatment, the cells were washed twice with 0.9 % NaCl. Subsequently, 691 μL of cold 50 mM Tris buffer (pH 7.5, Trizma base (Sigma-Aldrich, T1503)) was added. The protein was collected on ice and homogenized with an injection needle (26G×1/2) (TERUMO, NN-2613S) which was used for IAP measurement. IAP activity was measured using 1.25 mg/mL disodium p-nitrophenol phosphate as a substrate in Tris-HCl buffer (pH 10.0, 5 mM $MgCl_2.6H_2O$ (Wako, 135-00165) and 200 mM Trizma base (Sigma-Aldrich, T1503)), following a 30 min incubation at 37℃.

### *2.9. Preparation of Rat Intestinal Mucosal Protein*

The intestinal mucosal proteins were obtained from 5-week-old male Wistar rats (Japan SLC, Hamamatsu, Japan). Following a 12 h fast, the rats were anesthetized and the upper part of the small intestine was removed, cut open, and washed with cold saline. Subsequently, the small intestinal mucosal tissue was collected and the membrane proteins were extracted using Extraction Buffer 2B of the ProteoExtract® Transmembrane Protein Extraction Kit (Novagen, 71772) according to the manufacturer's protocol. The Ethics Committee on Animal Experiments at Gifu University approved all the experimental protocols performed (permit number: 15124). All experiments used in this study were performed in accordance to the experimental guidelines and regulations of Gifu University.

### *2.10. Preparation of Intestinal Lipid Rafts from Caco-2 Cells*

Caco-2 cells were treated with or without 2 mM IIAEK for 24 h. Following treatment, the cells were washed twice with ice-cold phosphate-buffered saline and collected in 1 mL of cold TNE buffer (25 mM Tris-HCl, 150 mM NaCl, 1 mM EGTA, pH 7.5) + 1% (w/v) Triton X-100. The cell lysates were homogenized on ice using a glass homogenizer (WHEATON, 903475) with an attached potter-type shuttle (WHEATON, 358034). The homogenate was transferred to the 13PA tube (HITACHI: 332001A), and 2 mL of 80% (w/v) sucrose in TNE buffer was added. They were layered with 6 mL of

 doi:10.20944/preprints202008.0055.v1



sucrose density gradient solution (5%~30%) using a fractionator and ultracentrifuged at 200,000×g at 4℃ for 17 h in an ultracentrifuge (himac, CP80WX, HITACHI) with swing rotor (himac, P40ST, HITACHI), as described previously [17]. Subsequently, they were fractionated into 10 fractions and recovered using the density gradient fractionator MODEL DGF-U (HITACHI). Sucrose density gradient formation was confirmed by measuring the sucrose density (w/w %) of each fraction with the ATAGO pocket sugar meter (ATAGO). Each fraction was subjected to ultrafiltration using an Amicon® Ultra 10K device (Millipore) according to the manufacturer's protocol. The concentrated protein solutions obtained were used for photoaffinity labeling.

### *2.11. Photoaffinity Labeling*

DMSO (0.5 μL) was added to rat intestinal mucosal protein fractions or intestinal lipid rafts from Caco-2 cells at the rate of 1 mg/mL, and incubated on ice for 15 min. Subsequently, 10 mM IIXEK (0.5 μL) dissolved in DMSO was added and incubated on ice for 15 min. Photoaffinity labeling was performed as described previously [18]. The protein fractions and lipid rafts were then subjected to UV irradiation at 365 nm for 30 min, and 302 nm for 10 min. Later, 2.5 μL of 10% SDS and 0.5 μL of 5 mM Azide-fluor488 (Sigma-Aldrich) were added. Next, 2 μL of the catalytic mixture (1.5 μL of 1.7 mM TBAT (TCI), 0.5 μL of 50 mM CuSO4 (Sigma-Aldrich), 0.5 μL of 50 mM Sodium L-ascorbate (Sigma-Aldrich)) was added and incubated at 32℃ for 30 min. Subsequently, this mixture was subjected to 10% SDS-PAGE for fluorescence scanning. BenchMark™ Fluorescent Protein Standard was used as the molecular weight marker.

### *2.12. SiRNA Experiments*

SiRNA experiments were performed as described previously [19]. Caco-2 cells were seeded in 6-well Transwell® plates (Corning, Inc., USA) at a density of $2\times10^5$ cells/well and grown for 8 h pre-confluence. Subsequently, 2.5 μL of siLentFectTM Lipid Reagent (BIO RAD, 170-3361) was diluted with 61 μL of serum-free DMEM. Therein, 61.2 μL of serum-free DMEM containing 285 nM IAP siRNA (Silencer® Select Pre-designed siRNA Product, Ambion, 4392420) or 285 nM Control siRNA (Silencncer® Select Negative Control #1 siRNA, Ambion, 439084) was mixed in equal amounts and incubated at room temperature for 20 min to generate siRNA-siLentFect complexes. Caco-2 cells were added to 122 μL of each siRNA-siLentFect complex and incubated for 48 h for transfection. After 48 h from transfection, total RNA was isolated for the determination of mRNA levels.

### *2.13. Statistical Analysis*

Values are expressed as means ± SEM. The statistical significance of the differences between two groups was evaluated by Student's *t*-tests [20]. The differences were considered significant when *p<0.05, **p<0.01, ***p<0.001.

## 3. Results

### *3.1. Effect of IIAEK on an Intestinal Cholesterol Absorption in Caco-2 Cells*

First, we measured the effect of IIAEK on intestinal cholesterol absorption in Caco-2 cells. Treatment of Caco-2 cells with 2 mM IIAEK resulted in a significant reduction in intestinal cholesterol absorption (Control: 100.0 ± 4.2 vs IIAEK 79.5 ±12.0, *p<0.05) (Figure 1A).

### *3.2. Effect of IIAEK on the mRNA Levels of Cholesterol Metabolism-Associated Genes in Caco-2 Cells*

To explore the mechanisms of intestinal cholesterol absorption via IIAEK at the genetic level, we investigated if IIAEK affected intestinal cholesterol metabolism-associated genes like Scavenger Receptor Class B Member 1 (SR-B1), Niemann-pick C1-like 1 L1 (NPC1L1), ATP-binding cassette transporter A1 (ABCA1), Acyl-coenzyme A: cholesterol acyltransferase 2 (ACAT2), Microsomal triglyceride transfer protein (MTP), ATP Binding Cassette Subfamily G Member 5 (ABCG5), ATP-binding cassette sub-family G member 8 (ABCG8), Cytochrome P450, family 27, subfamily A,

Preprints (www.preprints.org) | NOT PEER-REVIEWED | Posted: 3 August 2020 doi:10.20944/preprints202008.0055.v1



polypeptide 1 (CYP27A1), Liver X Receptor α (LXRα), and Liver X Receptor β (LXRβ) in differentiated Caco-2 cells. The cells were treated with 2 mM IIAEK or vehicle for 24 h. Compared to the control, 2 mM IIAEK significantly reduced the mRNA levels of SR-B1, ABCA1, ACAT2, MTP, CYP27A1, and LXRα in differentiated Caco-2 cells cultured with cholesterol micelle (SR-B1: Control, 12.81 ± 1.320 vs. IIAEK, 8.572 ± 0.7522; ABCA1: Control, 11.67 ± 1.515 vs. IIAEK, 6.808 ± 0.4138; ACAT2: Control, 14.50 ± 1.283 vs. IIAEK, 10.14 ± 0.9367; MTP: Control, 17.89 ± 2.689 vs. IIAEK, 9.987 ± 1.104; CYP27A1: Control, 14.68± 2.186 vs. IIAEK, 8.907 ± 1.373; LXRα: Control, 0.001695 ± 0.0001122 vs. IIAEK, 0.001080 ± 0.00006337; *p<0.05, ***p<0.001) (Figure 1B). 2 mM IIAEK also tended to decrease the mRNA level of LXRβ in the Caco-2 cells (LXRβ: Control, 0.001163 ± 0.0001037 vs. IIAEK, 0.0008079 ± 0.0001205; p = 0.08108) (Figure 1B).

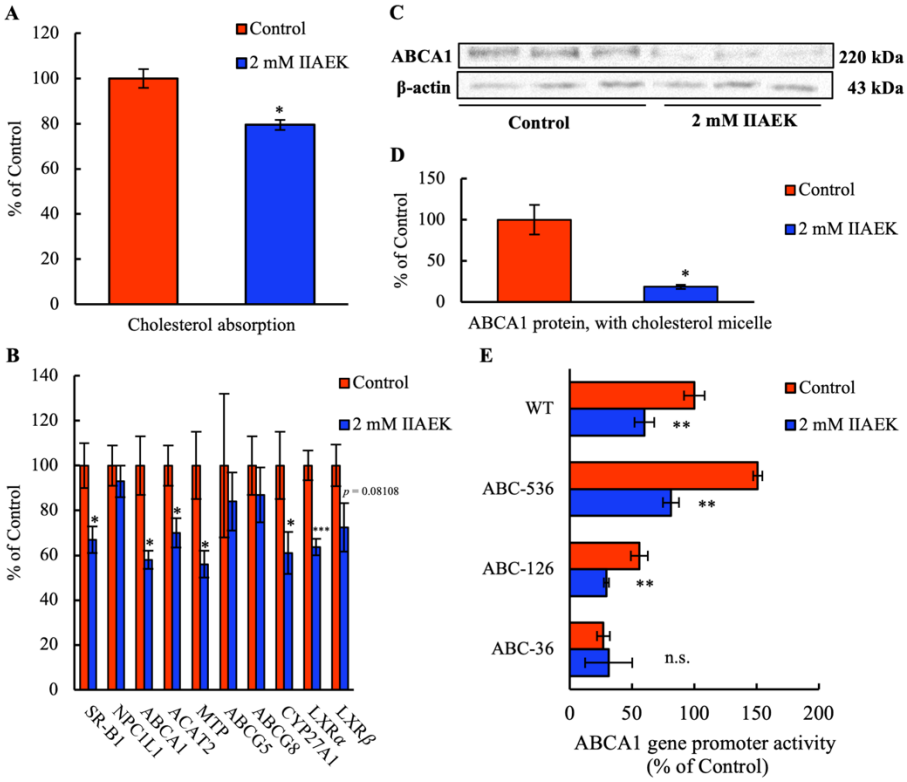


**Figure 1.** Effect of IIAEK containing cholesterol micelle on cholesterol metabolism in Caco-2 cells. (A) Effect of IIAEK containing cholesterol micelle on cholesterol absorption rate in Caco-2 cells. (B) Effect of IIAEK containing cholesterol micelle on cholesterol metabolism-associated gene expression in Caco-2 cells. Values are represented as means ± standard errors, represented by vertical bars (n = 6 per group). (C) Effect of IIAEK containing cholesterol micelle on ABCA1 protein level in Caco-2 cells by western blot. (D) ABCA1 protein level was quantified with ImageJ and normalized to the level of β-actin. Values are represented as mean ± standard error, represented by vertical bars (n = 3 per group). (E) Effect of IIAEK containing cholesterol micelle on ABCA1 gene promoter activity in Caco-2 cells. Caco-2 cells were transfected with the human pGK3-ABCA1-Luc plasmid (WT: −928 to +107 bp) or the pGK3-ABCA1-Luc plasmid deletion mutants (ABC−536: −536 to +107 bp, ABC−126: −126 to +107 bp, ABC−36: −36 to +107 bp), using the pGK β-galactosidase plasmid as an internal control. Data are presented as luciferase activity normalized to β-galactosidase activity. Values are represented as means ± standard error, represented by vertical bars (n = 5-9 per group). Asterisks indicate the difference from the control (*p < 0.05, ** p < 0.01), as determined by Student's t-test.

 doi:10.20944/preprints202008.0055.v1



*3.3. Effect of IIAEK on ABCA1 Protein Level in Caco-2 Cells*

We measured the effect of IIAEK on ABCA1 protein level in Caco-2 cells to evaluate if IIAEK affects intestinal ABCA1 protein and mRNA levels. Caco-2 cells were treated with or without 2 mM IIAEK for 48 h, and the cell lysate was subjected to Western blot analysis. We found that, compared to the control, treatment with 2 mM IIAEK significantly reduced the ABCA1 protein level in Caco-2 cells (Control: 1.881 ± 0.3378 vs. IIAEK: 0.3491 ± 0.04822, *p<0.05) (Figure 1C, D).

*3.4. Effect of IIAEK on ABCA1 Gene Promoter Activity in Caco-2 Cells*

We investigated the effect of IIAEK on human ABCA1 gene promoter activity in Caco-2 cells. We also used three deletion mutants of the ABCA1 gene promoter (ABC−536, ABC−126, ABC−36) to identify the important ABCA1 gene promoter region for the downregulation of ABCA1 by IIAEK. Caco-2 cells were treated with or without 2 mM IIAEK for 12 h, and the cell lysate was subjected to a luciferase assay. We found that treatment with 2 mM IIAEK significantly reduced ABCA1 gene promoter activity and the deletion of LXR and SP1 response region (ABC−36) of the ABCA1 gene promoter disappeared the decrease in ABCA1 gene promoter activity by IIAEK compared to the control (WT; Control: 24.19 ± 2.039 vs. IIAEK: 14.49 ± 1.927, ABC−536; Control: 36.49 ± 2.069 vs. IIAEK: 19.64. ± 3.553, ABC−126; Control: 13.51 ± 1.408 vs. IIAEK: 7.123 ± 0.4039, ABC−36; Control: 6.538 ± 1.020 vs. IIAEK: 7.484 ± 3.711, **p<0.01, n.s.: not significance) (Figure 1E).

*3.5. Chemical Synthesis of IIXEK, a Molecular Probe for Photoaffinity Labeling*

We used photoaffinity labeling to capture the target proteins interacting with IIAEK. Photoaffinity labeling involves the reversible interaction of a bioactive compound (e.g. IIAEK) with its target protein. The bioactive compound and target protein are mixed, irradiated with light, and a molecular probe with a photoreactive group is used to crosslink the bioactive compound and target protein with an irreversible covalent bond, thereby labeling them with fluorescent molecules. The click reaction was used to detect the target protein-IIAEK complex, following photoaffinity labeling using photoreactive groups. As described previously [18,21], we combined a diazirine moiety for target protein capture and a terminal alkyne for detecting the target protein complex to synthesize 3-ethynyl-5-[3-(trifluoromethyl)-3H-diazirin-3-yl] benzoic acid. Finally, we evaluated a site for introducing the chemically synthesized molecular probe into IIAEK. In our previous studies, we evaluated the effects of IIAEK, its fragment peptides and constituent amino acids, on CYP7A1 mRNA and found that the EK site was important for the bioactive effect of IIAEK [6]. Therefore, we retained the EK site and introduced the probe into the closest alanine residue at the EK site. However, since the alanine residue lacked an amino group, it was replaced with (S)-2,3-diaminopropionic acid. The probe was introduced into the side chain amino group of (S)-2,3-diaminopropionic acid by the formation of an amide bond (Figure 2A). The synthesized probe was consigned to Peptide Institute, Inc. (Japan). Thus, IIXEK, a mutant form of IIAEK possessing 3-ethynyl-5-[3-(trifluoromethyl)-3H-diazirin-3-yl] benzoic acid was synthesized by a 9-fluorenylmethyloxycarbonyl (Fmoc) strategy (Figure 2B). Upon UV irradiation, this IIXEK forms covalent bonds with the target proteins (Figure 2B). Furthermore, to confirm the occurrence of the click reaction, rhodamine was introduced into IIXEK with diazirine and terminal alkyne in the presence of a copper ion catalyst. Subsequently, we tested for the occurrence of the Huisgen cycloaddition reaction (Figure 2C). The click reaction began at room temperature. At 1 h post reaction initiation, the analysis was performed using LC-MS (JEOL, JMS-T100TD, Instrumental Analysis Field, Gifu University Life Science Research Support Center). The peak arising due to click reaction was detected at m/z 1397.82 $[M-H]^-$ (Figure 2D).

Preprints (www.preprints.org) | NOT PEER-REVIEWED | Posted: 3 August 2020 doi:10.20944/preprints202008.0055.v1



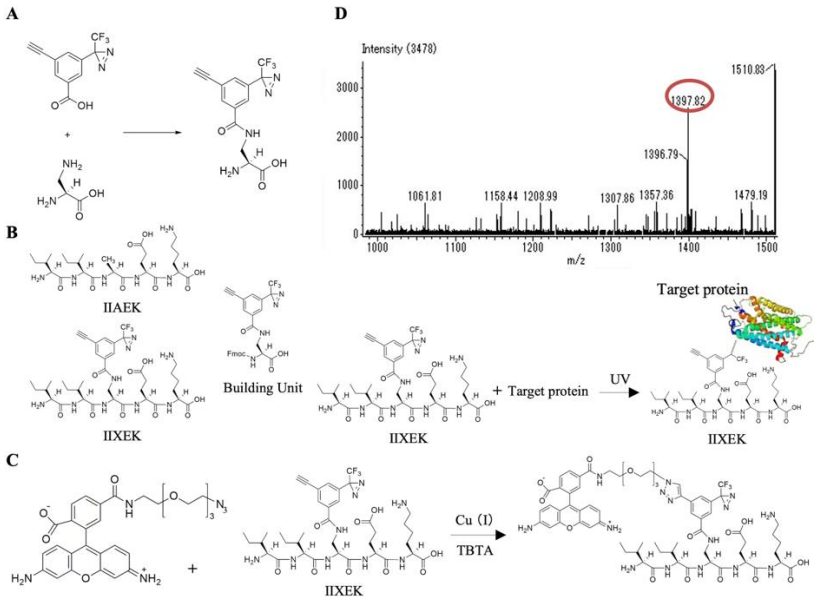


**Figure 2.** Chemical synthesis of the molecular probe, IIXEK. (A) Amide bond by 3-ethynyl-5-[3-(trifluoromethyl)-3H-diazirin-3-yl] benzoic acid and (S)-2,3-diaminopropionic acid. (B) Structure of IIXEK. IIXEK possesses chemically synthesized 3-ethynyl-5-[3-(trifluoromethyl)-3H-diazirin-3-yl] benzoic acid. This probe captures the target proteins interacting with IIAEK. (C) Click reaction, which occurs by introduction of rhodamine into IIXEK in the presence of copper as catalyst (Huisgen cycloaddition reaction). (D) Mass spectrometry of Cu-Catalyzed Azide (Azide-fluor 488) Alkyne (IIXEK) cycloaddition.

*3.6. Photoaffinity Labeling and MS Analysis of the Intestinal Lipid Raft Fractions Derived from Caco-2 Cells and Rat Intestinal Mucosal Protein by a Novel Molecular Probe, IIXEK*

We showed that IIAEK decreased intestinal cholesterol absorption in Caco-2 cells by downregulating the expression of intestinal cholesterol metabolism-associated genes (Fig. 1A and B). Based on these results, we hypothesized that IIAEK might affect the expression of intestinal cholesterol metabolism-associated genes in Caco-2 cells by an intracellular signaling. Therefore, we focused on lipid rafts as a signaling platform and developed an experimental method to extract intestinal lipid rafts of Caco-2 cells according to a sucrose density gradient. The level of flotillin-1, a lipid raft marker protein, was measured. The findings revealed that it was clustered in fraction (Fr.) 2 to 4 (Figure 3A, B). We also measured the specific enzyme activity of IAP, another lipid raft marker, and found a peak in the specific activity of IAP in Fr. 3 and 4 (Figure 3C). Compared to the control group, treatment with 2 mM IIAEK was found to about 3-fold increase the specific activity of IAP (Figure 3C). We performed photoaffinity labeling and MALDI-TOF mass spectrometry (MS) analysis (AXIMA Performance, SHIMADZU)) of IIXEK on Fr. 3 and found that human IAP, a target molecule, interacted with IIAEK in the 86.8 kDa band (Figure 3D). Also, our previous animal studies revealed that IIAEK exhibited a greater hypocholesterolemic activity compared to beta-sitosterol. Thus, we performed photoaffinity labeling and MS analysis on the rat small intestinal mucosal proteins using IIXEK to capture the target proteins interacting with IIAEK. We found that IAP-1 and IAP-2, presented in a fluorescent band at 94.1 kDa, were target proteins interacting with IIAEK (Figure 3E). Interestingly, comparison of the IIXEK-binding amino acid sequences of IAP in the rat small intestinal mucosal protein fractions (IAP-1, IAP-2) (Figure 3E) and intestinal lipid raft fraction of Caco-2 cells (IAP) (Figure 3D) by MS analysis revealed that GFYLFVEGGR was the common IIAEK-binding amino acid sequence, and their position within rat IAP-1 (P15693) from N to C terminal: 325-334 or IAP-2 (P51740) from 324-333, and human IAP (P09923) from 324-333.

Preprints (www.preprints.org) | NOT PEER-REVIEWED | Posted: 3 August 2020 doi:10.20944/preprints202008.0055.v1



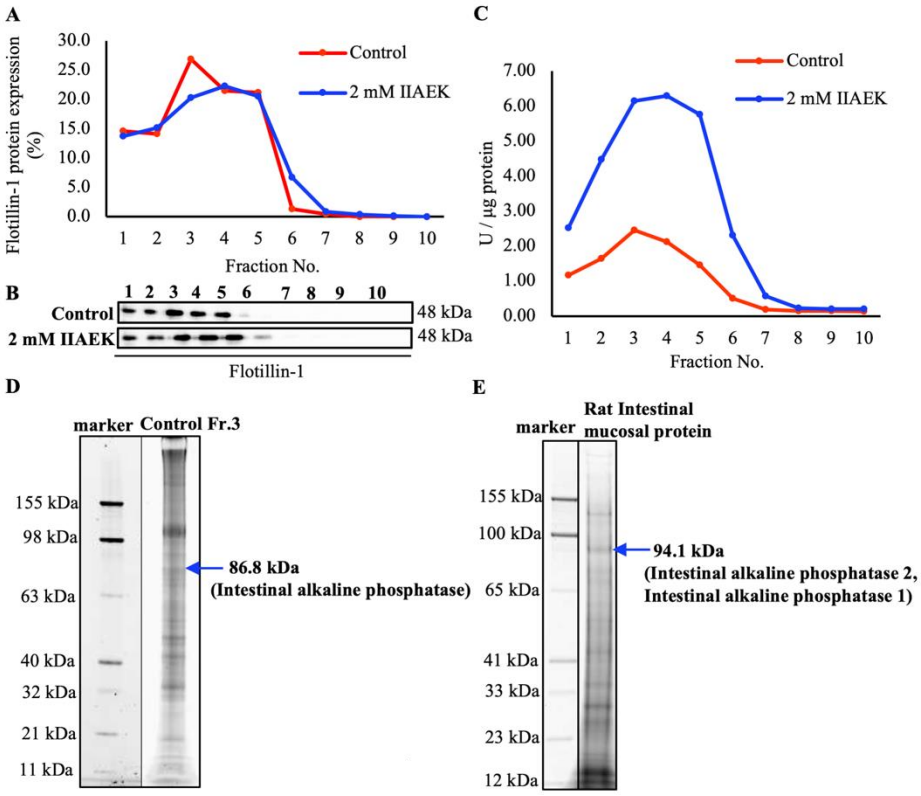


**Figure 3.** Extraction of intestinal lipid raft fractions from Caco-2 cells and photoaffinity labeling by IIXEK for the lipid raft fraction and rat intestinal mucosal protein.
(A, B) Protein level of the lipid raft marker flotilin-1 in each fraction. (C) IAP specific activity of the lipid raft marker in each fraction. (D) Photoaffinity labeling of intestinal lipid raft proteins by IIXEK. The intestinal lipid raft fraction (Fr. 3) containing 250 μM IIXEK was irradiated with UV for 30 min for photoaffinity labeling. Subsequently, the fraction containing the fluorescent substance, rhodamine, which was added by a click reaction, was separated on SDS-PAGE. (E) Photoaffinity labeling of rat intestinal mucosal protein fractions by IIXEK. We collected the small intestinal mucosal proteins of 5-week-old male Wister rats. The membrane protein fractions, which were derived from rat small intestinal mucosa, were collected with EB2B of TM-PEK and made into rat small intestinal mucosal fractions. Photoaffinity labeling was performed in the same way as described in Fig. 3D.

*3.7. IIAEK Induces IAP Activation and Down-Regulation of ABCA1 in Caco-2 Cells*

Caco-2 cells were treated with 2 mM IIAEK or vehicle for 24 h. Compared to the control, IIAEK significantly increased the specific activity of IAP in Caco-2 cells incubated with or without cholesterol micelle (Without cholesterol micelle: Control 0.0648 ± 0.0005 vs. IIAEK 0.0706 ± 0.0003, ***p<0.001; With cholesterol micelle: Control 0.0668 ± 0.0005 vs. IIAEK 0.0699 ± 0.0003, ***p<0.001) (Figure 4A, B). Moreover, IIAEK significantly increased the IAP mRNA level in Caco-2 cells incubated with or without cholesterol micelle, compared to the control (Without cholesterol micelle: Control 1.0117 ± 0.0707 vs. IIAEK 1.3704 ± 0.0833, **p<0.01; With cholesterol micelle: Control 1.0086 ± 0.0600 vs. IIAEK 1.2018 ± 0.0527, *p<0.05) (Figure 4C, D). We also investigated the mRNA level of the cholesterol metabolism-associated gene, ABCA1. IIAEK significantly reduced the ABCA1 mRNA level in Caco-2 cells incubated with or without cholesterol micelle, compared to the control (Without cholesterol micelle: Control 1.0275 ± 0.1107 vs. IIAEK 0.7096 ± 0.0180, *p<0.05; With cholesterol micelle: Control 1.0066 ± 0.0518 vs. IIAEK 0.7959 ± 0.0175, **p<0.01) (Figure 4E, F). In addition, in Caco-2 cells incubated without cholesterol micelle, IIAEK significantly increased IAP protein level (Control: 1.127 ± 0.302 vs. IIAEK: 1.650 ± 0.237, *p<0.05) (Figure 4G, H) and decreased ABCA1 protein level compared to the control (Control: 1.706 ± 0.160 vs. IIAEK: 1.203 ± 0.119, *p<0.05) (Figure 4I, J).

Preprints (www.preprints.org) | NOT PEER-REVIEWED | Posted: 3 August 2020 doi:10.20944/preprints202008.0055.v1



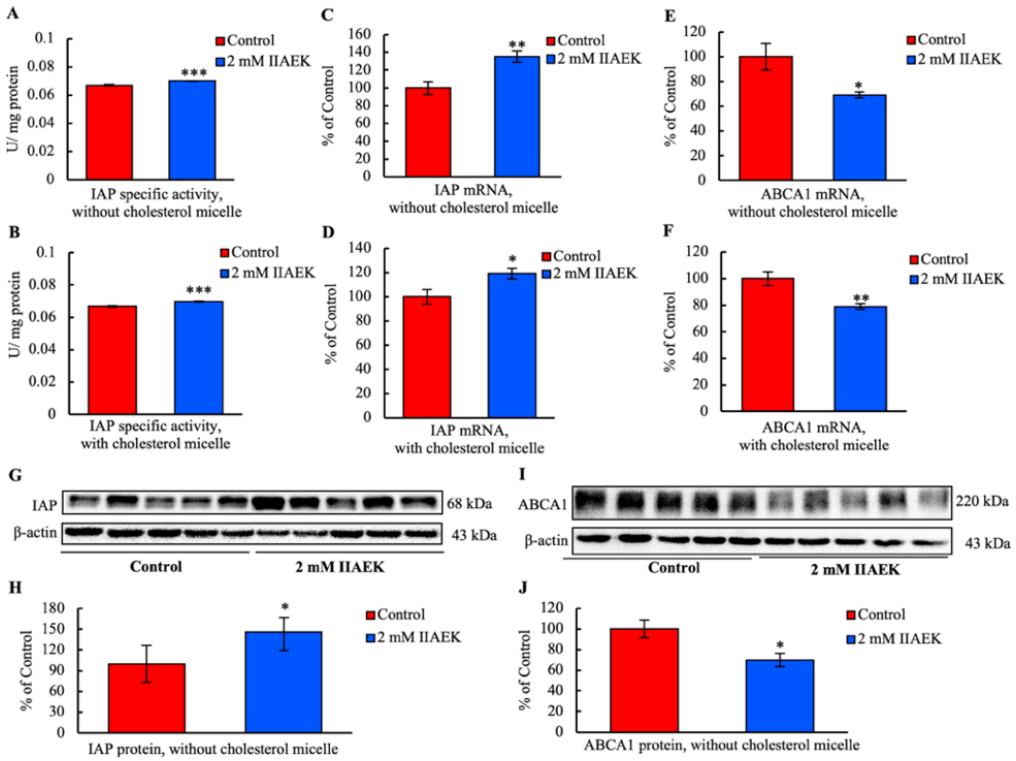


**Figure 4.** Effects of IIAEK on the expression of IAP and the cholesterol metabolism-associated gene, ABCA1. Caco-2 cells were cultured in 6-well Transwell plates. The cells were treated with serum-free medium containing 2 mM IIAEK or vehicle for 24 h. They were incubated with or without cholesterol micelle. (A, B) The total proteins were collected from the cells and the specific activity of ALP was measured. Values are represented as means ± standard error represented by vertical bars (n = 6 per group). (C-F) Total RNA was collected from the cells. The IAP and ABCA1 mRNA levels were measured by real-time PCR and normalized to the mRNA expression level of 18S ribosomal RNA. Values are represented as means ± standard error represented by vertical bars (n = 6 per group). (G, I) The cell lysate was collected from the cell, separated on SDS-PAGE, and analyzed by Western blot analysis. (H, J) The IAP and ABCA1 protein levels were quantified with ImageJ and normalized to the level of β-actin. Values are represented as means ± standard error represented by vertical bars (n = 5 per group). Asterisks indicate the difference from the control (*$p < 0.05$, **$p < 0.01$, ***$p < 0.001$) as determined by Student's t-test.

### *3.8. Relationship between IAP and ABCA1 in Caco-2 Cells*

IAP has been known to be associated with lipid metabolism. However, no reports are available on the relationship between IAP and cholesterol metabolism-associated genes. Therefore, we tested the relationship between IAP and ABCA1, a cholesterol metabolism-associated gene. We measured the ABCA1 mRNA level in Caco-2 cells when IAP mRNA level was significantly decreased by the introduction of the IAP siRNA-siLentFect complex. The IAP mRNA level was significantly reduced in Caco-2 cells cultured with IAP siRNA-siLentFect complex for 8 h compared to a 20 nM control siRNA group (20 nM control siRNA: 1.001 ± 0.030 vs. 20 nM IAP siRNA: 0.678 ± 0.053, **p<0.01) (Figure 5A). Moreover, the significant change in IAP mRNA level counteracted a decrease in the ABCA1 mRNA level (20 nM control siRNA: 1.002 ± 0.030 vs. 20 nM IAP siRNA: 1.023 ± 0.068, not significant) (Figure 5B**)**.

Preprints (www.preprints.org) | NOT PEER-REVIEWED | Posted: 3 August 2020 doi:10.20944/preprints202008.0055.v1



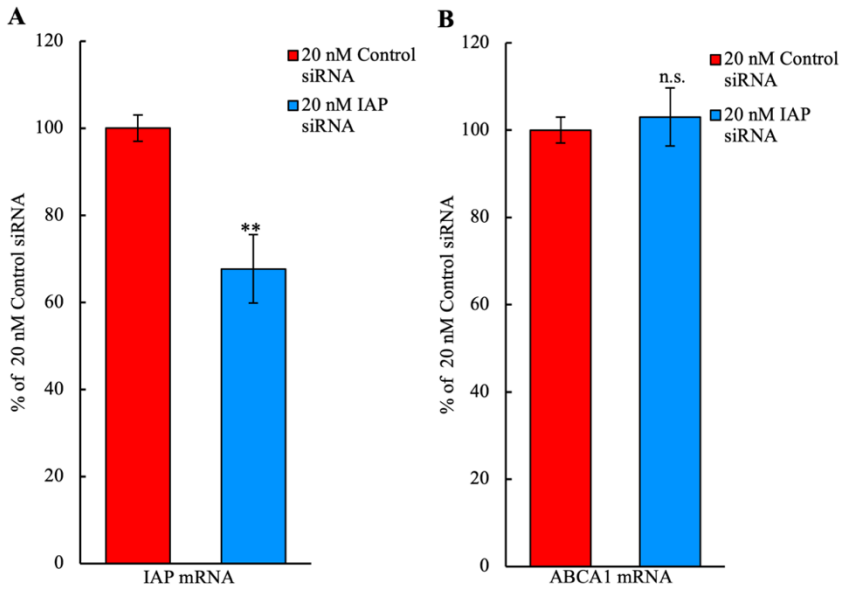


**Figure 5.** IAP and ABCA1 mRNA levels in Caco-2 cells introduced with IAP siRNA or Control siRNA. Caco-2 cells were cultured on 6-well Transwell plates for 8 h. Thereafter, 20 nM IAP siRNA-siLentFect complex or 20 nM Control siRNA-siLentFect complex was introduced into the cells and incubated for 48 h. (A, B) Total RNA was isolated from the cells, and IAP or ABCA1 mRNA levels were measured by real-time PCR and normalized to the mRNA expression level of 18S ribosomal RNA. Values are represented as means ± standard error represented by vertical bars (n = 3 per group). Asterisks indicate the difference from the control (**$p < 0.01$, n.s.: not significance) as determined by Student's t-test.

## 4. Discussion

We found that the cholesterol-lowering pentapeptide IIAEK affects various intestinal cholesterol metabolism-related genes (SR-B1, ABCA1, ACAT2, and MTP) in Caco-2 cells with an inhibitory effect of cholesterol absorption and, in particular, significantly decreases the protein level and promoter activity of ABCA1 (Figure 1A–E). Based on Figure 1B-D, as 27-OH cholesterol is a ligand for LXR, we presume that the significant decrease in the mRNA level of CYP27A1 by IIAEK may reduce 27-OH cholesterol to decrease LXR$\alpha$ mRNA, mRNA and protein levels of ABCA1 [22]. Therefore, to identify the important ABCA1 promoter site for the downregulation of ABCA1 by IIAEK, we conducted the luciferase assay by use of deletion mutants of ABCA1 promoter (Figure 1E). We found that the deletion of LXR and SP1 response area of ABCA1 promoter disappears the decrease in ABCA1 promoter activity by IIAEK (Figure 1E). Take all together, Figure 1B and E shows the decrease in the mRNA level of ABCA1 by IIAEK may be involved in LXR response element. Intestinal ABCA1 functions as a regulator of cholesterol absorption [23]. Interestingly, a recent study has shown that cholesterol absorption reduces by ~28% and total plasma cholesterol reduces by approximately 30% in intestinal ABCA1 KO mice [23]. Our study has shown that a reduction in the intestinal ABCA1 expression level was associated with the suppression of intestinal cholesterol absorption by a novel cholesterol-lowering dipeptide, phenylalanine-proline (FP) [12]. These results suggest that IIAEK exerts an inhibitory effect on cholesterol absorption which is accompanied by a decrease in the expression of ABCA1 in Caco-2 cells.

There is no information about food-derived bioactive peptide related specific receptor including IIAEK. For the first time, we identified the target proteins interacting with IIAEK on the surface of the small intestinal epithelial cells using a novel molecular probe, IIXEK. IIXEK was synthesized chemically and transfected with fluorescent substances to visualize the target protein complex interacting with the photoaffinity-labeled IIAEK (Figure 2A-D). Photoaffinity labeling and MS analysis of the small intestinal mucosal protein fractions of rats were performed using IIXEK. Lipid raft fractions extracted from Caco-2 cells were also subjected to photoaffinity labeling and MS

 doi:10.20944/preprints202008.0055.v1



analysis (Figure 3D). Human IAP was detected in the 86.8 kDa band. IAP is a brush border enzyme highly expressed in the small intestine [24]. Humans possess at least four isotypes of ALP: tissue nonspecific ALP (TNAP), which is expressed in the liver, bone, and kidney; intestinal ALP (IAP), which is localized in the small intestine; placental ALP (PALP); and germ cell ALP (GCAP) [25]. ALP, including IAP, is a glycoprotein, and ALP contains about 20% carbohydrate [26]. Although all ALPs are encoded by the same mRNA, depending on their location in the intestine, they may undergo various glycosylation processes [27]. Previous studies have revealed that the molecular weight of rat IAP was 93 kDa [28,29].

The molecular weight of the novel molecular probe IIXEK, used in this photoaffinity labeling experiment, is 0.82387 kDa, and IIXEK forms irreversible covalent bonds with target proteins upon UV irradiation. We have discovered there is the common IIAEK binding amino acid sequence (GFYLFVEGGR) of IAP in both Caco-2 cells and rat intestine. Therefore, it was suggested that one IIXEK molecules (0.82387 kDa) bound to the 93 kDa rat IAP and the band of the rat IAP-IIXEK complex was detected around 93.82387 kDa by SDS-PAGE. Subsequently, we studied the target molecules interacting with IIAEK in the lipid raft fraction extracted from Caco-2 cells. Previous reports have shown that a 5% SDS-PAGE gel can detect a human IAP subunit at 86 kDa, and gel filtration can detect a human IAP dimer at 170 kDa [30]. Since human IAP contains one common IIXEK-binding sequence in each subunit, we suggested that a single IIXEK molecule (0.82387 kDa) binds to the 86 kDa human IAP. In addition, we also detected a band of the human IAP-IIXEK complex at around 86.82387 kDa on a SDS-PAGE gel. While, in the rat small intestinal mucosal fractions, IAP1 and IAP2, the intestinal alkaline phosphatases (IAP), were detected in the 94.1 kDa band (Figure 3E).

ALP including IAP occurs in two forms: first, as a GPI-anchored protein [31,32] and second, as a secreted protein (non GPI-anchored protein) [31]. The GPI-anchored protein is a receptor that covalently binds to glycosylphosphatidylinositol (GPI), a saturated phospholipid. GPI-anchored protein resides in a signaling microdomain called lipid raft, which is present in the plasma membrane [33]. For example, the GPI-anchored protein CD59, a dimer, forms a stable tetramer following extracellular ligand stimulation, leading to the induction of intracellular signaling molecules associated with the GPI-anchored protein, resulting in intracellular signaling ($IP_3$-$Ca^{2+}$) [33]. In mice, the GPI-anchored protein CD55 regulates osteoclast function through receptor activator-associated Rac signaling of NF-κβ ligands [34]. Only few studies have reported on GPI-anchored IAP-mediated signaling. However, as GPI-anchored proteins like CD59 [33] and CD55 [34] regulate physiological functions via intracellular signaling, the existence of a novel signaling system mediated by GPI-anchored IAP is highly probable. Interestingly, our results verify the existence of a novel signaling pathway associated with the interaction of IIAEK with IAP, which is expressed at high levels in the small intestine.

We compared the IIXEK-binding amino acid sequence of IAP in the rat small intestinal mucosal protein fraction with that of the intestinal lipid raft fraction of Caco-2 cells. Surprisingly, GFYLFVEGGR was found to be the common amino acid binding sequence of IIAEK for IAP. This common amino acid sequence was also found in Akp3, one of the murine IAPs. The glutamic acid (E) in this sequence is coordinated by $Mg^{2+}$ in the rat IAP, along with aspartic acid (D), the 42$^{nd}$ amino acid residue, serine (S) the 155$^{th}$, and glutamine (Q) the 317$^{th}$ residue. The serine residue forms the active center of the rat IAP. Rat IAPs are coordinated by three metal ions, one $Mg^{2+}$ and two $Zn^{2+}$, which play an important role in the enzyme activity [35]. However, the physiological and biochemical implications and the affinity of the IIAEK common amino acid binding amino acid sequence (GFYLFVEGGR) for IAPs obtained from rat small intestinal mucosal proteins and Caco-2 cell-derived intestinal lipid raft fractions, and the amino acid sequence interacting with IIAEK are issues that need to be investigated in the future.

Since our experimental results have suggested that IIAEK upregulates IAP expression and downregulates ABCA1 expression via GPI-anchored IAP, we focused on the association between IAP and ABCA1. Our findings reveal that the IAP mRNA level of Caco-2 cells is significantly reduced following incubation with 20 nM IAP siRNA for 8 h under culture conditions, and that this decrease

 doi:10.20944/preprints202008.0055.v1



counteracted a decrease in the ABCA1 mRNA level (Figure 5A, B). The transcription factors that bind to the IAP promoter include HNF-4$\alpha$ [36], KLF5 [37], TR-RXR$\alpha$ heterodimer [38], ZBP-89 [39], and Cdx-1 [40], and the transcription factors of ABCA1 include LXR/RXR (transcriptional activation), TR$\beta$/RXR (transcriptional suppression), and SREBP-2 [22]. The existence of a common transcription factor that binds to both IAP and ABCA1 gene promoter is highly likely. However, further investigations are needed to determine if IIAEK affects this common transcription factor.

Our results show that IIAEK significantly increases IAP mRNA, protein levels and enzyme activity significantly decreases ABCA1 mRNA and protein levels, both of which are cholesterol absorption-associated genes (Figure 3A, 3C, 4A-J). The physiological functions of IAP are associated with the regulation of homeostasis in the small intestinal epithelial environment, and includes fatty acid absorption in the small intestine [41], detoxification of inflammatory mediators by dephosphorylation [42,43], pH regulation of the duodenal surface [44], inhibition of LPS-induced inflammatory responses [24], and regulation of the tight junction-associated proteins at the genetic level [45]. Interestingly, IAP is closely associated with lipid metabolism. Previous studies have suggested that the increased absorption of fatty acids and serum triglycerides in the small intestine in IAP KO mice is related to the fatty acid transporter CD36, which is present in the vicinity of Akp6, one of the murine IAPs [46]. Further studies on the molecular mechanisms are necessary to understand the relationship between IAP and lipid metabolism.

In our previous study, we reported a significant increase in the serum HDL cholesterol level and a significant decrease in the serum LDL+VLDL cholesterol level in rats administered IIAEK orally compared to the casein tryptic hydrolysate (CTH) group [3]. In particular, a significant reduction in total serum cholesterol levels was observed in rats administered IIAEK orally compared to beta-sitosterol [3]. Our current experimental findings reveal that the addition of 2 mM IIAEK significantly increases the IAP mRNA and protein levels, and IAP specific activity of Caco-2 cells incubated with or without cholesterol micelle. Based on previous reports and our current experimental findings, we propose that IAP is involved in cholesterol metabolism, which is crucial for improving and preventing lifestyle diseases like atherosclerosis and myocardial infarction.

Interestingly, IAP KO mice show symptoms of metabolic disorders like elevated plasma cholesterol level, elevated serum triglyceride level and abnormal glucose tolerance [47]. IAP has been shown to prevent aging, contribute to prolonged lifespan, target the intestinal barrier, and improve the disruption of intestinal permeability in mice [48]. Oral administration of IAP significantly decreases serum triglyceride and LDL-cholesterol levels and significantly increases serum HDL-cholesterol level in mice [47,48]. However, no reports exist on the relationship between GPI-anchored IAPs and cholesterol metabolism. Most reports of IAPs associated with lipid metabolism only have discussed the functions of IAPs secreted as non GPI-anchored IAPs [31].; few research groups have focused on the functions of GPI-anchored IAPs [31,32]. Although the existence of a close association between IAP and lipid metabolism has been proposed, only few reports have discussed the relationships between IAP and cholesterol metabolism. Our findings reveal a novel signaling pathway involving IIAEK, a ligand which interacts with GPI-anchored IAPs to induce intracellular signaling, thereby upregulating IAP mRNA and protein levels, and downregulating ABCA1 mRNA and protein levels, accompanied by the inhibition of cholesterol absorption. We have particularly emphasized that IAP is a novel target molecule in the regulation of cholesterol metabolism.

## 5. Conclusions

In conclusion, IIAEK interacts with GPI-anchored IAP which is highly expressed in the small intestinal epithelial cells, and improves cholesterol metabolism through the upregulation of IAP and downregulation of ABCA1 via the intracellular signaling (Figure 6). Our findings contribute to the elucidation of the physiological response of oligopeptides on the cell membrane, and the intracellular signal transduction pathways associated with cholesterol metabolism.

Preprints (www.preprints.org) | NOT PEER-REVIEWED | Posted: 3 August 2020 doi:10.20944/preprints202008.0055.v1



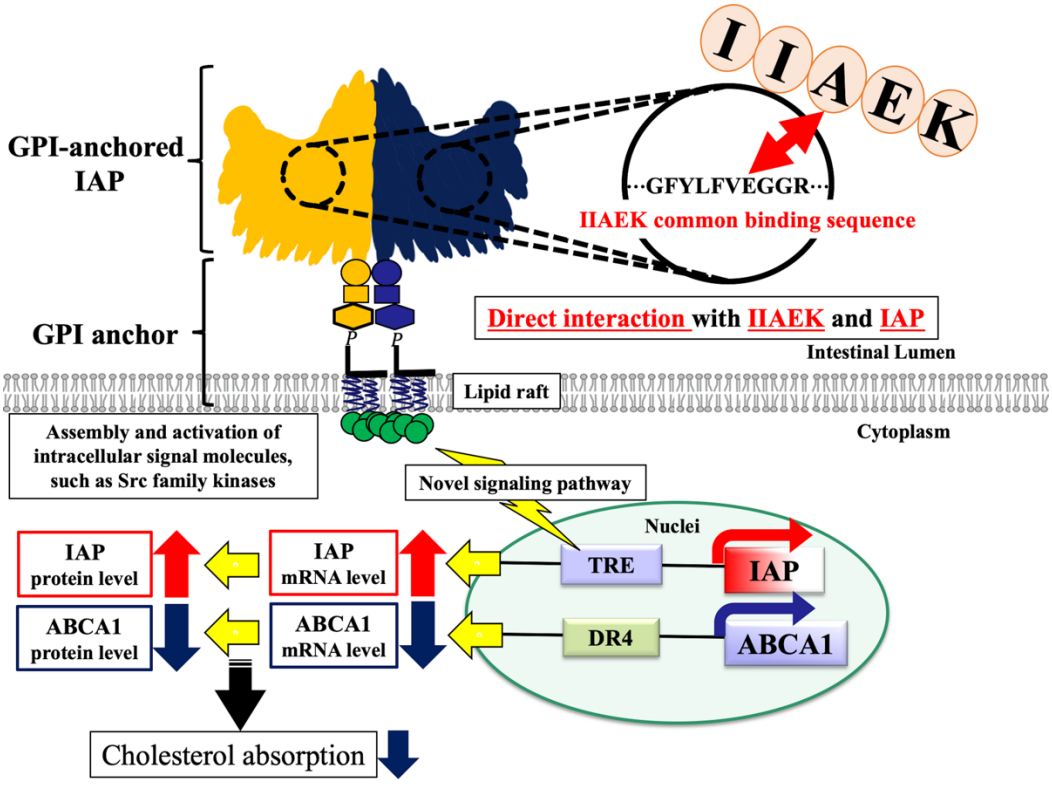


**Figure 6.** IIAEK-IAP interaction hypothesis. IIAEK interacts with IAP and improves cholesterol metabolism by the specific activation of IAP and downregulation of intestinal ABCA1.

**Author Contributions:** S.N. developed the study design and wrote the manuscript; A.T., K.H., N.O., Y.S., E.Y. and Y.U. conducted the research and contributed to the manuscript. All authors have read and approved the final manuscript.

**Acknowledgments:** The authors are grateful to Taguchi, Y., Sakai, Y., Komuro, A., Yamamoto, T., and Hoshi, M. at Gifu University for their technical assistance. This study was supported in part by a Grant-in-Aid for Scientific Research from the Japanese Ministry of Education, Culture, Sports, Science and Technology (No. 17H00817 to S.N.).

**Conflicts of Interest:** The authors declare no competing interests.

## References

1. Ginsberg, H.N.; Barr, S.L.; Gilbert, A.; Karmally, W.; Deckelbaum, R.; Kaplan, K.; Ramakrishnan, R.; Holleran, S.; Dell, R.B. Reduction of plasma cholesterol levels in normal men on an American Heart Association step 1 diet or a step 1 diet with added monounsaturated fat. *N. Engl. J. Med.* **1990**, *322*, 574–579.
2. Hori, G.; Wang, M.F.; Chan, Y.C.; Komatsu, T.; Wong, Y.; Chen, T.H.; Yamamoto, K.; Nagaoka, S.; Yamamoto, S. Soy protein hydrolysate with bound phospholipids reduces serum cholesterol levels in hypercholesterolemic adult male volunteers. *Biosci. Biotechnol. Biochem.* **2001,** *65*, 72–78.
3. Nagaoka, S.; Futamura, Y.; Miwa, K.; Awano, T.; Yamauchi, K.; Kanamaru, Y.; Kojima, T.; Kuwata, T. Identification of novel hypocholesterolemic peptides derived from bovine milk β-lactoglobulin. *Biochem. Biophys. Res. Commun.* **2001**, *281*, 11-17.
4. Spady, D.K.; Cuthbert, J.A.; Willard, M.N.; Meidell, R.S. Adenovirus- mediated transfer of a gene encoding cholesterol 7α- hydroxylase into hamsters increases hepatic enzyme activity and reduces plasma total and low density lipoprotein cholesterol. *J. Clin. Invest*., **1995**, *96*, 700–709.
5. Spady, D.K.; Cuthbert, J.A.; Willard, M.N.; Meidell, R.S. Overexpression of cholesterol 7α-hydroxylase (CYP7A) in mice lacking the low density lipoprotein (LDL) receptor gene. LDL transport and plasma LDL concentrations are reduced. *J. Biol. Chem*., **1998**, *273*, 126–132.
6. Morikawa, K.; Kondo, I.; Kanamaru, Y.; Nagaoka, S. A novel regulatory pathway for cholesterol degradation via lactostatin. *Biochem. Biophys. Res. Commun.*, **2007**, *352*, 697–702.

7. Singh, A.; Thornton, E.R.; Westheimer, F.H. The photolysis of diazoacetylchymotrypsin. *J. Biol. Chem.*, **1962**, *237*, 3006–3008.
8. Tomohiro, T.; Hatanaka, Y. Diazirine-based multifunctional photo-probes for affinity- based elucidation of protein-ligand interaction. *Heterocycles*, **2014**, *89*, 2697– 2727.
9. Kolb, H.C.; Finn, M.G.; Sharpless, K.B. Click chemistry: diverse chemical function from a few good reactions. *Angew. Chem. Int. Ed.*, **2001**, *40*, 2004–2021.
10. Rostovtsev, V.V.; Green, L.G.; Fokin, V.V.; Sharpless, K.B. A stepwise huisgen cycloaddition process: Copper (I)-catalyzed regioselective "Ligation" of azides and terminal alkynes. *Angew. Chem. Int. Ed.*, **2002**, *41*, 2596– 2599.
11. Tornøe, C.W.; Christensen, C.; Meldal, M. Peptidotriazoles on solid phase: [1,2,3]-triazoles by regiospecific copper (I)-catalyzed 1,3-dipolar cycloadditions of terminal alkynes to azides. *J. Org. Chem.*, **2002**, *67*, 3057–3064.
12. Banno, A.; Wang, J.; Okada, K.; Mori, R; Maihemuti, M; Nagaoka, S. Identification of a novel cholesterol-lowering dipeptide, phenylalanine-proline (FP), and its down-regulation of intestinal ABCA1 in hypercholesterolemic rats and Caco-2 cells. *Sci. Rep.* **2019**, *9*, 19416.
13. Field, F.J.; Watt, K.; Mathur, S.N. TNF-$\alpha$ decreases ABCA1 expression and attenuates HDL cholesterol efflux in the human intestinal cell line Caco-2. *J. Lipid Res.*, **2010**, *51*, 1407–1415.
14. Kitamura, K.; Okada, Y.; Okada, K.; Kawaguchi, Y.; Nagaoka, S. Epigallocatechin gallate induces an up-regulation of LDL receptor accompanied by a reduction of PCSK9 via the annexin A2-independent pathway in HepG2 cells. *Mol. Nutr. Food. Res.*, **2017**, *61*, 1600836.
15. Noda, S.; Yamada, A.; Nakaoka, K.; Goseki-sone, M. 1-alpha, 25-Dihydroxyvitamin $D_3$ up-regulates the expression of 2 types of human intestinal alkaline phosphatase alternative splicing variants in Caco-2 cells and may be an important regulator of their expression in gut homeostasis. *Nutr Res*., **2017**, *46*, 59-67.
16. Ilboudo, S.; Fouche, E.; Rizzati, V.; Toè, A.M.; Gamet-Payrastre, L.; Guissou, P.I. In vitro impact of five pesticides alone or in combination on human intestinal cell line Caco-2. *Toxicol. Rep.* **2014**, *1*, 474-489.
17. Yuyama, K.; Sekino-Suzuki, N.; Sanai, Y.; Kasahara, K. Translocation of activated heterotrimeric G protein G$\alpha$o to ganglioside-enriched detergent-resistant membrane rafts in developing cerebellum. *J. Biol. Chem.*, **2007**, *282*, 26392-26400.
18. Nakamoto, K.; Akao, Y.; Ueno, Y. Diazirine-containing tag-free RNA probes for efficient RISC-loading and photoaffinity labeling of microRNA targets. *Bioorganic Med. Chem. Lett.*, **2018**, *28*, 2906–2909.
19. Zanka, K.; Kawaguchi, Y.; Okada, Y.; Nagaoka, S. Epigallocatechin gallate induces upregulation of LDL receptor via the 67 kDa laminin receptor-independent pathway in HepG2 cells. *Mol. Nutr. Food. Res.*, **2020**, *64*, 1901036.
20. Snedecor, G.W; Cochran, W.G. In: Statistical Methods, 6th ed. Ames: The Iowa State University Press., **1967**.
21. Hosoya, T.; Hiramatsu, T.; Ikemoto, T.; Aoyama, H.; Ohmae, T.; Endo, M.; Suzuki, M. Design of dantrolene-derived probes for radioisotope-free photoaffinity labeling of proteins involved in the physiological $Ca^{2+}$ release from sarcoplasmic reticulum of skeletal muscle. *Bioorganic Med. Chem. Lett.* **2005**, *15*, 1289–1294.
22. Schmitz, G.; Langmann, T. Transcriptional regulatory networks in lipid metabolism control ABCA1 expression. *Biochim. Biophys. Acta.*, **2005**, *1735*, 1–19.
23. Iqbal, J.; Parks, J.S.; Hussain, M.M. Lipid absorption defects in intestine-specific microsomal triglyceride transfer protein and ATP-binding cassette transporter A1- deficient mice. *J. Biol. Chem.*, **2013**, *288*, 30432–30444.
24. Goldstein, D.J.; Rogers, C.E.; Harris, H. Expression of alkaline phosphatase loci in mammalian tissues. *Proc. Natl. Acad. Sci. USA.*, **1980**, *77*, 2857–2860.
25. Lallès, J.P. Recent advances in intestinal alkaline phosphatase, inflammation, and nutrition. *Nutr. Rev.*, **2019**, *77*, 710–724.
26. Yedlin, S.T.; Young, G.P.; Seetharam, B.; Seetharam, S.; Alpers, D.H. Characterization and comparison of soluble and membranous forms of intestinal alkaline phosphatase from the suckling rat. *J. Biol. Chem.*, **1981**, *256*, 5620–5626.
27. Sogabe, N.; Mizoi, L.; Asahi, K.; Ezawa, I.; Goseki-Sone, M. Enhancement by lactose of intestinal alkaline phosphatase expression in rats. *Bone*, **2004**, *35*, 249–255.
28. Xie, Q.M.; Zhang, Y.; Mahmood, S.; Alpers, D.H. Rat intestinal alkaline phosphatase Ⅱ messenger RNA is present in duodenal crypt and villus cells. *Gastroenterology*, **1997**, *112*, 376-386.

29. Malik, N.; Butterworth, P.J. Molecular properties of rat intestinal alkaline phosphatase. *Biochim. Biophys. Acta.*, **1976**, *446*, 105–114.
30. Hirano, K.; Sugiura, M.; Miki, K.; Iino, S.; Suzuki, H.; Oda, T. Characterization of Tissue-specific Isozyme of Alkaline Phosphatase from Human Placenta and Intestine. *Chem. Pharm. Bull.* **1977**, *25*, 2524–2529.
31. Nakano, T.; Inoue, I.; Alpers, D.H.; Akiba, Y.; Katayama, S.; Shinozaki, R.; Kaunitz, J.D.; Ohshima, S.; Akita, M.; Takahashi, S.; *et al.* Role of lysophosphatidylcholine in brush-border intestinal alkaline phosphatase release and restoration. *Am. J. Physiol. Gastrointest. Liver Physiol.* **2009**, *297*, 207–214.
32. Harada, T.; Koyama, I.; Sato, K.; Komoda, T. Induction of rat alkaline phosphatase isozymes bearing a glycan-phosphatidylinositol anchor modified by in vivo treatment with a benzimidazole derivative linked to ethylbenzene. *Comp. Biochem. Physiol., Part B: Biochem. Mol. Biol.*, **2000**, *127*, 193–202.
33. Suzuki, K.; Kasai, R.; Hirosawa, K.; Nemoto, Y.; Ishibashi, M.; Miwa, Y.; Fujiwara, T.; Kusumi, A. Transient GPI-anchored protein homodimers are units for raft organization and function. *Nat. Chem. Biol.* **2012**, *8*, 774–783.
34. Shin, B.; Won, H.; Adams, D.J.; Lee, S.K. CD55 regulates bone mass in mice by modulating RANKL-mediated Rac signaling and osteoclast function. *J. Bone Miner. Res.*, **2020**, *35*, 130–142.
35. Ghosh, K.; Tagore, D.M.; Anumula, Lakshmaiah, B.; Kumar, P.P.B.S.; Singaram, S.; Matan, T.; Kallipatti, S.; Selvam, S.; Krishnamurthy, P.; *et al.* Crystal structure of rat intestinal alkaline phosphatase – Role of crown domain in mammalian alkaline phosphatase. *J. Struct. Biol.* **2013**, *184*, 182–192.
36. Olsen, L.; Bressendorff, S.; Troelsen, J.T.; Olsen, J. Differentiation-dependent activation of the human intestinal alkaline phosphatase promoter by HNF-4 in intestinal cells. *Am. J. Physiol. Gastrointest. Liver Physiol.*, **2005**, *289*, 220–226.
37. Shin, J.; Carr, A.; Corner, G.A.; Tögel, L.; Dávaos-Salas, M.; Tran, H.; Chueh, A.C.; Al-Obaidi, S.; Chionh, F.; Ahmad, N.; *et al.* The intestinal epithelial cell differentiation marker intestinal alkaline phosphatase (ALPi) is selectively induced by histone deacetylase inhibitors (HDACi) in colon cancer cells in a Kruppel-like Factor 5 (KLF5)- dependent manner. *J. Biol. Chem.* **2014**, *289*, 25306–25316.
38. Malo, M.S.; Zhang, W.; Alkhoury, F.; Pushpakaran, P.; Abedrapo, M.A.; Mozumder, M.; Fleming, E.; Siddique, A.; Henderson, J.W.; Hodin, R.A. Thyroid hormone positively regulates the enterocyte differentiation marker intestinal alkaline phosphatase gene via an atypical response element. *Mol. Endocrinol.* **2004**, *18*, 1941–1962.
39. Malo, M.S.; Mozumder, M.; Zhang, X.B.; Biswas, S.; Chen, A.; Bai, L.; Merchant, J.L.; Hodin, R.A. Intestinal alkaline phosphatase gene expression is activated by ZBP-89. *Am. J. Physiol. Gastrointest. Liver Physiol.* **2006**, *290*, 737–746.
40. Alkhoury, F.; Malo, M.S.; Mozumder, M.; Mostafa, G.; Hodin, R.A. Differential regulation of intestinal alkaline phosphatase gene expression by Cdx1 and Cdx2. *Am. J. Physiol. Gastrointest. Liver Physiol.*, **2005**, *289*, 285–290.
41. Narisawa, S.; Huang, L.; Iwasaki, A.; Hasegawa, H.; Alpers, D.H.; Millán J.L. Accelerated fat absorption in intestinal alkaline phosphatase knockout mice. *Mol. Cell. Biol.* **2003**, *23*, 7525–7530.
42. Chen, K.T.; Malo, M.S.; Moss, M.S.; Zeller, S.; Johnson, P.; Ebrahimi, F.; Mostafa, G.; Alam, S.N.; Ramasamy, S.; Warren, H.S.; *et al.* Identification of specific targets for the gut mucosal defense factor intestinal alkaline phosphatase. *Am. J. Physiol. Gastrointest. Liver Physiol.* **2010**, *299*, 467–475.
43. Moss, A.K.; Hamarneh, S.R.; Mohamed, M.M.R.; Ramasamy, S.; Yammine, H.; Patel, P.; Kaliannan, K.; Alam, S.N.; Muhammad, N.; Moaven, O.; *et al.* Intestinal alkaline phosphatase inhibits the proinflammatory nucleotide uridine diphosphate. *Am. J. Physiol. Gastrointest. Liver Physiol.* **2013**, *304*, 597-604.
44. Mizumori, M.; Ham, M.; Guth, P.H.; Engel, E.; Kaunitz, J.D.; Akiba, Y. Intestinal alkaline phosphatase regulates protective surface microclimate pH in rat duodenum. *J. Physiol.* **2009**, *587*, 3651–3663.
45. Liu, W.; Hu, D.; Huo, H.; Zhang, W.; Adiliaghdam, F.; Morrison, S.; Ramirez, J.M.; Gul, S.S.; Hamarneh, S.R.; Hodin, R.A. Intestinal alkaline phosphatase regulates tight junction protein levels. *J. Am. Coll. Surg.* **2016**, *222*, 1009–1017.
46. Lynes, M.D.; Widmaier, E.P. Involvement of CD36 and intestinal alkaline phosphatases in fatty acid transport in enterocytes, and the response to a high-fat diet. *Life Sci.*, **2011**, *88*, 384–391.
47. Kaliannan, K.; Hamarneh, S.R.; Economopoulos, K.P.; Alam, S.N.; Moaven, O.; Patel, P.; Malo, N.S.; Ray, M.; Abtahi, S.M.; Muhammad, N.; *et al.* Intestinal alkaline phosphatase prevents metabolic syndrome in mice. *Proc. Natl. Acad. Sci. USA.* **2013**, *110*, 7003–7008.

 doi:10.20944/preprints202008.0055.v1



48. Kühn, F.; Adiliaghdam, F.; Cavallaro, P.M.; Hamarneh, S.R.; Tsurumi, A.; Hoda, R.S.; Munoz, A.R.; Dhole, Y.; Ramirez, J.M.; Liu, E.; *et al.* Intestinal alkaline phosphatase targets the gut barrier to prevent aging. *JCI Insight* **2020**, *5*, e134049.